CHAPTER 7

Automated Poultry Carcass Inspection by a Hyperspectral–Multispectral Line-Scan Imaging System

Kuanglin Chao

US Department of Agriculture, Agricultural Research Service, Henry A. Wallace Beltsville Agricultural Research Center, Environmental Microbial and Food Safety Laboratory, Beltsville, Maryland, USA

CONTENTS

7.1. INTRODUCTION

Hyperspectral imaging is one of the latest technologies to be developed for effective and non-destructive quality and safety inspection in the area of food processing. The technology takes the most useful characteristics of both machine vision and spectroscopy, two technologies already widely used in the food and agricultural industries. *Machine vision* imaging is commonly used to detect surface features (color, size/shape, surface texture, or defects) in food inspection, but cannot identify or detect chemical, biological, or material properties or characteristics from the product. In contrast, *spectroscopy* can evaluate these properties and characteristics, but does not provide the spatial information that is often critical in food inspection. *Hyperspectral imaging* integrates the main features of imaging and spectroscopy to simultaneously acquire both spectral and spatial information, which is key to evaluating food safety and quality attributes. As a result, the technology provides us with unprecedented detection capabilities, which otherwise cannot be achieved with either imaging or spectroscopy alone. Hyperspectral imaging technology has been a proven tool for developing methods of

Hyperspectral Imaging for Food Quality Analysis and Control

CONTENTS

automated multispectral inspection (Kim *et al.*, 2001; Lu & Chen, 1998). However, one major limiting factor that initially hindered direct commercial application of hyperspectral technology for on-line use was the speed needed for rapid acquisition and processing of large-volume hyperspectral image data (Chen *et al.*, 2002; Gowen *et al.*, 2007). More recently, advanced computer and optical sensing technologies are gradually overcoming this problem, as demonstrated by the development of on-line hyperspectral detection systems for inspection of poultry carcasses for wholesomeness and fecal contamination (Chao, Chen *et al.*, 2002; Lawrence, Park *et al.*, 2003; Lawrence, Windham *et al.*, 2003; Park *et al.*, 2002), inspection of apples for fecal contamination (Kim *et al.*, 2002, 2004; Mehl *et al.*, 2002), and sorting and grading of fruits for internal quality (Lu & Peng, 2006; Noh & Lu, 2007; Qin & Lu, 2006). In particular, the line-scan imaging technology has demonstrated significant advantages for the direct implementation of hyperspectral imaging for rapid automated food quality and safety inspection such as on-line poultry inspection (Chao *et al.*, 2007; Yang *et al.*, 2009).

The Agricultural Research Service (ARS), an agency of the United States Department of Agriculture (USDA), has had a long-term interest in developing automated inspection methods for food and agricultural products. Beginning in the 1960s and continuing to this day, ARS research on spectroscopy and spectral imaging methods for non-destructive food quality and safety measurement has included the development of visible/near-infrared (VIS/NIR) techniques for grain and oilseed quality, for fruit and vegetable quality, for food quality and safety of dairy, meat, and poultry. The first computerized NIR spectrophotometer was developed by ARS researchers and ultimately led to the now widespread use of the technology in the grain industry. Current ongoing research includes the development of automated spectral imaging for the detection of surface contaminants on fresh produce and for wholesomeness inspection and contamination detection on poultry carcasses, all on high-speed processing lines.

This chapter describes the development of automated chicken inspection techniques by ARS researchers that has led to the latest hyperspectral line-scan imaging system for wholesomeness inspection on commercial high-speed processing lines, which is now under commercial development for industrial use. In addition to the usual problems inherent to the fundamental research for developing feasible spectral methods to assess poultry characteristics, researchers also had to address significant challenges in adapting the scientific findings to implement them in the current ARS imaging system for practical real-world use in automated high-speed processing environments. The current USDA poultry inspection program and the progression of

ARS VIS/NIR spectroscopy methods, target-imaging, and hyperspectral/multispectral line-scan imaging for poultry inspection are discussed in the following sections.

7.2. CURRENT UNITED STATES POULTRY INSPECTION PROGRAM

The 1957 Poultry Product Inspection Act (PPIA) mandates post-mortem inspection of every bird carcass processed by a commercial facility for human consumption. Since then, the USDA has employed inspectors from its Food Safety and Inspection Service (FSIS) agency to conduct on-site organoleptic inspection of all chickens processed in poultry plants in the United States for indications of disease or defect conditions. At inspection stations on commercial evisceration lines, FSIS inspectors examine by sight and by touching the body, the inner body cavity surfaces, and the internal organs of every chicken carcass on the evisceration line (USDA, 2005). Most chicken plants in the United States operate evisceration lines at speeds of 70 birds per minute (bpm) or 91 bpm, using either a Streamlined Inspection System (SIS) or a New Line Speed (NELS) inspection system. Additionally, some newer high-speed chicken processing systems operate evisceration lines at even higher speeds, as high as 140 bpm. By law, the human inspectors may work at a maximum speed of 35 bpm, which results in multiple inspection stations along a single line. In this way, for example, one inspector examines every fourth chicken on a 140 bpm line and the line is equipped with four inspection stations in the USDA inspection zone (Figure 7.1).

Poultry processing plants in the United States process over 8.9 billion broilers (young chickens, 4–6 weeks old) annually, more than any other country and valued at over $31 billion (USDA, 2008). Broiler production has increased dramatically over the years to meet rising market demand. The domestic per capita consumption of broilers increased from 27 kg in 1990 to 34.9 kg in 2000, and reached 39.5 kg in 2006. Currently, about 2200 FSIS poultry inspectors are employed to inspect roughly 8.9 billion broilers per year. With ever-increasing consumer demand for poultry products, human inspection capability is becoming the limiting factor to increased production throughput.

The inspection program implemented by FSIS as a result of the 1957 PPIA addresses mandatory inspection of poultry products for food safety only, not for quality attributes. Products that pass this safety inspection are labeled as having been USDA Inspected and Passed. The human inspectors are trained to visually and manually inspect poultry carcasses and viscera

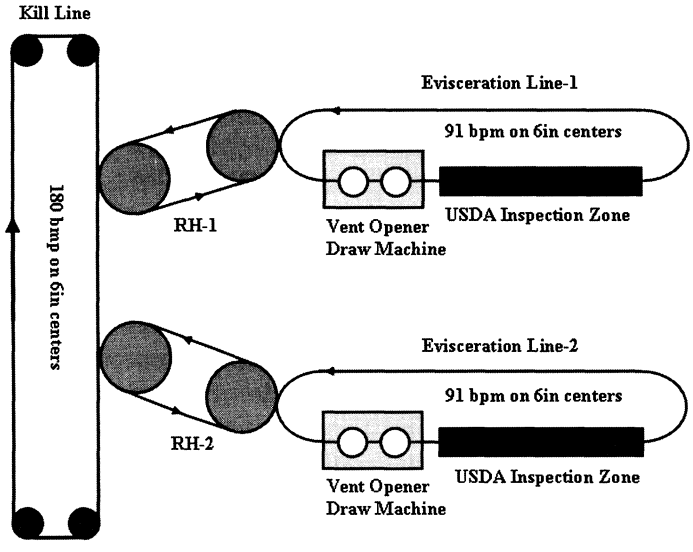

FIGURE 7.1 *Diagram of poultry processing lines, including a 180 bpm Kill Line, two Re-Hangers (RH), and two 91 bpm Evisceration Lines. Inspection stations are located in the USDA Inspection Zones on the Evisceration Line. (Full color version available on http://www.elsevierdirect.com/companions/9780123747532/)*

on-line at processing plants to accurately identify unwholesome carcasses, including those exhibiting conditions such as septicemia/toxemia (septox), airsacculitis, ascites, cadaver, and inflammatory process (IP), and defects such as bruises, tumors, sores, and scabs. This inspection process is subject to human variability, and also makes inspectors prone to developing fatigue and repetitive motion injuries.

With advances in science and improved food safety awareness, USDA food safety programs have seen further developments during the past two decades. With the 1996 final rule on Pathogen Reduction and Hazard Analysis and Critical Control Point (HACCP) systems (USDA, 1996), FSIS implemented the HACCP and Pathogen Reduction programs in meat and poultry processing plants throughout the country to prevent food safety hazards. HACCP systems for food safety focus on prevention and monitoring of potential hazards at critical control points throughout a food production process, instead of focusing only on product safety inspection. FSIS has also been testing the HACCP-Based Inspection Models Project (HIMP) in a few volunteer plants (USDA, 1997). In this project, food safety performance standards are set by FSIS and the processing plants bear primary responsibility for conducting inspections and processing so that their products satisfy FSIS standards, while FSIS inspectors perform carcass verification along and

at the end of the processing line, before the birds enter the final chill step. FSIS inspectors no longer perform bird-by-bird inspection in these volunteer HIMP plants, which number 20 plants out of over 400 federally inspected plants nationwide.

7.3. DEVELOPMENT OF VIS/NIR SPECTROSCOPY-BASED POULTRY INSPECTION SYSTEMS

Since the early 1990s, significant advances have occurred in the development of automated poultry inspection systems. Leading research in this area has been done by USDA Agricultural Research Service (ARS) scientists, originally initiated by an FSIS request to ARS to develop methods for addressing issues in high speed poultry inspection. Methods based on visible/near-infrared (VIS/NIR) reflectance spectroscopy were first investigated as a tool for identifying carcass conditions based on spectral measurements. This initial work resulted in both spectroscopy-based on-line inspection systems and also selective filter-based multispectral imaging systems for identifying poultry conditions.

7.3.1. Spectral Analysis Using Laboratory-based Photodiode-array Detection Systems

Information about the color, surface texture, and chemical constituents of chicken skin and muscle tissue is carried in VIS/NIR light reflected from a carcass. Because unwholesome carcasses that are diseased or defective often have a variety of changes in skin and tissue, these carcasses can be detected with VIS/NIR reflectance techniques that require no physical contact during data acquisition. A photodiode-array (PDA) VIS/NIR spectrophotometer system was first developed (Chen & Massie, 1993) to measure chicken spectra in the laboratory. The system used a bifurcated fiber-optic assembly for sample illumination and spectral reflectance measurement (471 nm to 964 nm), in conjunction with quartz–tungsten–halogen lamps to provide the illumination. The end of the probe was positioned approximately 2 cm from the chicken surface, a distance that was determined during laboratory experiments to optimize the signal-to-noise ratio for the spectral measurements. Spectra were measured for wholesome carcasses and septicemic/cadaver carcasses, with an acquisition time of 2 second for each stationary measurement.

Analysis using principal component analysis (PCA) achieved classification accuracies of 93.3% and 96.2% for the chicken samples in the

wholesome and unwholesome classes, respectively. Later experiments (Chen *et al.*, 1998) were conducted to measure the reflectance spectra of freshly slaughtered carcasses hung on track-mounted sliding shackles, to simulate processing line speeds of 60 and 90 bpm. The measurements were acquired for wholesome carcasses and for carcasses exhibiting symptoms of septicemia/toxemia, cadaver, airsacculitis, ascites, and tumors (these disease/defect conditions often cause birds to be removed from the processing line).

7.3.2. Pilot Scale On-line Photodiode-array Poultry Inspection System

Based on the laboratory PDA spectrophotometer system, a transportable pilot-scale VIS/NIR system (Chen *et al.*, 1995) was developed and taken to a chicken processing plant to conduct on-line VIS/NIR spectral measurements on a 70 bpm commercial evisceration line. Reflectance measurements were selectively triggered for individual wholesome and unwholesome carcasses specifically identified by a veterinary medical officer observing the birds on the processing line. Acquisition time for each spectral measurement was 0.32 s, targeting an area of approximately 10 cm^2 across the breast area of each bird as it passed in front of the fiber-optic probe.

Processing and analysis of the spectral data was performed off-line. Preprocessing of the 1024-point raw spectral data included smoothing by 9-point running mean and a second difference calculation. Reduction of the second difference spectra was performed by extracting every fifth point, producing 190-point spectra spanning 486.1 nm to 941.5 nm (2.4 nm spacing). PCA was performed on these reduced second difference spectra. The coefficients (PCA scores) of the first 50 principal components were used as inputs to a feed-forward back-propagation neural network for classification of the chicken carcasses. The neural network used 50 input nodes, seven nodes in a hidden layer, and two output nodes whose ideal output were either (0,1) or (1,0) to indicate wholesome or unwholesome bird condition. For the data set collected for 1750 chickens (1174 wholesome and 576 unwholesome) on the 70 bpm processing line, analysis resulted in an average classification accuracy of 95% (Chen *et al.*, 1998, 2000).

7.3.3. Charge-coupled Device Detector Systems for In-plant On-line Poultry Inspection

The VIS/NIR spectrophotometer system was updated to enable on-line chicken inspection at line speeds greater than 90 bpm. The PDA detection system was replaced with a charge-coupled device- (CCD-) based detection system, which allowed for much shorter data acquisition times for spectral

measurement (Chao *et al.*, 2003). Additionally, moving away from the Microsoft DOS-based software drivers of the PDA detector allowed researchers to use up-to-date software based on the Microsoft Windows operating system that provided greater flexibility and modularity to implement real-time on-line acquisition, processing, and classification algorithms.

Testing of the updated CCD-based VIS/NIR chicken inspection system (Figure 7.2) for in-plant on-line poultry inspection was conducted in commercial poultry plants at line speeds of 140 and 180 bpm. In-plant testing of this system was guided by specific FSIS food safety performance standards defined under HIMP. One specific HIMP food safety performance standard requires removal of any bird exhibiting the systemic disease conditions of septicemia or toxemia, which are characterized by pathogenic microorganisms or their toxins in the bloodstream. As a result, system testing targeted classification of 450 wholesome and 426 unwholesome (specifically, systemically diseased) birds that were selected by an FSIS veterinary medical officer observing birds on the processing line. A 1024-point spectrum was acquired across the range of 431–943 nm for each individual bird, using a total data acquisition time of 60 ms per bird in order to process an accumulation of three consecutive spectral measurements of 20 ms each. At 140 bpm, classification accuracies of 95% for wholesome and 92% for unwholesome birds were achieved. At 180 bpm, classification accuracies of 94% and 92% for wholesome and unwholesome birds were achieved, respectively (Chao *et al.*, 2004).

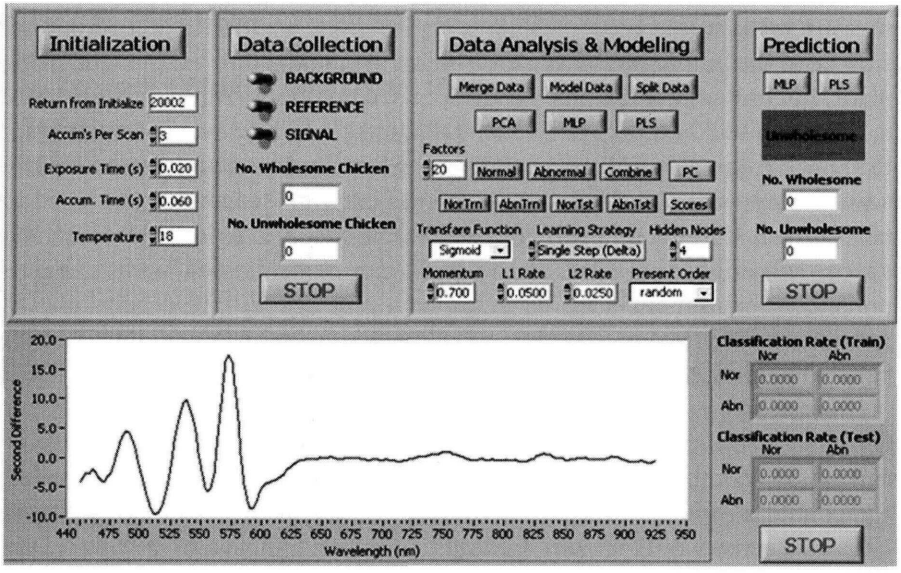

FIGURE 7.2

User interface of the CCD-based VIS/NIR chicken inspection system. (Full color version available on http://www.elsevierdirect.com/companions/9780123747532/)

7.3.4. Summary of Spectroscopy-based Poultry Inspection Systems

The spectroscopy-based inspection systems were designed to scan a limited area of each bird carcass, to measure the reflectance spectra in the VIS/NIR regions between 400 nm and 950 nm for detection of condemnable systemic disease conditions. In-plant testing demonstrated classification accuracies above 90% in differentiating wholesome and systemically diseased chickens. The upgrade from PDA- to CCD-based detection resulted in significantly improved data processing speeds due to the associated computer peripherals for data transfer. The use of CCD-based detection also provided significantly greater flexibility in the development of software controls for on-line inspection applications, especially for analysis algorithms such as neural network classification of spectra.

However, spectral classification utilizing the neural network approach requires a considerable volume of training data—e.g. in-plant on-line measurements of at least 500 wholesome and 500 unwholesome birds—in order for the classification model to reliably differentiate between wholesome and unwholesome birds. Because calibration is customized to a particular population of birds, re-calibration is necessary to accommodate different environmental and growth factors that affect bird condition (e.g. changes between seasons, diet) and processing variations between different processing plants (e.g. scalding parameters).

Consistent sample presentation is ideal for spectral classification—but difficult to achieve in the on-line processing environment. Ideally, spectral measurement would be performed with the probe positioned 2 cm from the surface of the bird breast, at the mid-breast area of the bird. In the processing plant, not only might there be variation in that probe-to-surface distance due to vibration and both forward/backward and side-to-side sway of the bird on the shackle, but also difficulty in using the fixed-position probe to accurately scan the mid-breast target area due to the external sensor system (used to trigger measurement for each bird) and variations in individual bird size and shape. Vibration and sway of the birds can be addressed with stability-enhancing equipment such as guide bars and synchronized belts on the processing line, but attempting to adjust probe position for bird-to-bird variations in size and shape would be an extremely difficult challenge.

Spectroscopy-based inspection using a fiber-optic probe is well suited for the commercial chicken processing environment since the probe assembly can be easily mounted on the line and can tolerate humidity and higher temperatures while the detector and computer system can be sheltered a short distance away within a climate-controlled enclosure. However, the

spectroscopy-based inspection system is limited to small area measurements across each bird, and not necessarily with precision targeting of the measurement area. Systemic disease conditions can be detected in this way, but problems affecting only localized portions of a bird carcass, such as inflammatory process (IP) or randomly located defects or contamination (bruises, tumors, and fecal contamination), cannot be effectively identified without whole-surface carcass inspection.

7.4. DEVELOPMENT OF TARGET-TRIGGERED IMAGING FOR ON-LINE POULTRY INSPECTION

Following initial ARS development of spectroscopy-based on-line inspection systems, subsequent improvements in computer technology and optical sensing devices made possible the development of laboratory-based multispectral and hyperspectral imaging systems. Formerly used primarily for remote sensing applications, hyperspectral imaging technology was adapted for small-scale laboratory experiments by ARS researchers and others, once off-the-shelf computer systems became able to handle the huge hyperspectral data volumes. These laboratory systems were used to analyze hyperspectral image data for the development of multispectral methods suitable for addressing specific inspection applications. The resultant multispectral methods, using a limited number of wavelengths, were applied for target-triggered on-line implementation in separate multispectral imaging systems due to imaging and processing speed restrictions imposed by hardware limitations.

7.4.1. Dual-camera and Color Imaging

Based on the work of Chen & Massie (1993), who analyzed VIS/NIR spectral data by PCA, an intensified multispectral imaging system using six optical filters (at 542, 570, 641, 700, 720, and 847 nm) and neural network classifiers was developed in the laboratory for discrimination of wholesome poultry carcasses from unwholesome carcasses that included septicemia/toxemia and cadaver carcasses (Park & Chen, 1994). The accuracy for separation of wholesome carcasses from unwholesome carcasses was 89.3%. Following these results, the textural features based on the co-occurrence matrix of the multispectral images were analyzed (Park & Chen, 1996). Because the 542 nm and 700 nm wavelengths were found to be significant in separating the wholesome and unwholesome birds, a dual-camera imaging system using interference filters was then assembled for testing on a laboratory pilot-scale processing line (Park & Chen, 2000). This dual-wavelength system used two

interference filters (20 nm bandpass), one centered at 540 nm and the other at 500 nm. Two black/white progressive scan cameras (TM-9701, PULNiX Inc., Sunnyvale, CA, USA) were positioned side-by-side, each fitted with one of the two filters. The dual-camera system acquired pairs of images for chickens on shackles moving at 60 bpm. Off-line image processing and input of the image intensity data to a feed-forward back-propagation neural network resulted in classification accuracies of 93.3% for the septicemia carcasses and 95.8% for cadaver carcasses (Chao *et al.*, 2000). At a commercial poultry processing plant, the dual-camera imaging system was used for on-line image acquisition on a 70 bpm evisceration line. The images of 13 132 wholesome and 1 459 unwholesome chicken carcasses were analyzed off-line and resulted in classification accuracies of 94% and 87% for wholesome and unwholesome carcasses, respectively (Chao, Chen *et al.*, 2002).

Symptoms of some unwholesome poultry conditions such as airsacculitis and ascites can be exhibited by the visceral organs of a bird. Since human inspectors on chicken processing lines often examine both the poultry viscera and the outer muscle and skin, chicken liver and heart samples were collected from wholesome carcasses and unwholesome septicemia, airsacculitis, and cadaver carcasses (40 birds for each of the four categories) to investigate the classification of bird condition based on color imaging of the viscera. With the available samples divided equally between training and validation data sets, combined color image features of the liver and heart for each individual bird were entered into a generalized neuro-fuzzy classification model that achieved 86.3% and 82.5% accuracies for the training and validation data sets, respectively (Chao *et al.*, 1999).

Although these results showed the potential of detecting individual diseases by color imaging of both carcass and visceral organs, this line of investigation was not developed further due to the relatively few plants using processing lines in which viscera and carcass can be suitably presented for imaging. Systems do exist in which the visceral organs are consistently presented on a tray alongside the carcass, but in most poultry plants, carcasses are hung on processing line shackles with the visceral organs automatically drawn and draped to the side in a randomly oriented manner.

7.4.2. Two-dimensional Spectral Correlation and Color Mixing

In general, the development of multispectral imaging techniques first requires analysis and selection of specific wavelengths to be implemented by said multispectral image techniques. Many studies have based wavelength selection on the use of chemometrics and multivariate analysis such as PCA. Alternative methods have also been investigated during the course of

developing multispectral imaging methods for chicken inspection, including two-dimensional spectral correlation (2-D correlation) and color mixing.

Myoglobin is the major pigment in well-bled muscle-tissue. The color of muscle tissue is largely determined by the relative amounts of three forms of myoglobin at the surface: deoxymyoglobin, oxymyoglobin, and metmyoglobin. Generally, deoxymyoglobin appears purplish; oxymyoglobin—an oxygenated form—appears bright red; and metmyoglobin—the oxidized form of the previous two—appears brownish. Liu & Chen (2000, 2001) applied a 2-D correlation technique to spectral data collected for chicken breast meat samples to investigate spectral differences related to chicken meat conditions. These studies examined the changes in myoglobin proteins that occur during meat degradation and storage processes, and identified spectral absorptions associated with the molecular vibrations of specific myoglobin species (i.e. measurable changes due to inter-species reactions affecting relative amounts of the myoglobin forms found in different meat conditions). It was also realized that spectral absorptions could be affected by unique molecular vibrations resulting from the interactions of these myoglobin species with surrounding meat components such as water and lipids, not just from the molecular vibrations of the myoglobin species themselves. Visible wavebands identified in association with these myoglobin species included bands near 545 nm and 560 nm with oxymyoglobin, 445 nm with deoxymyoglobin, and 485 nm with metmyoglobin.

The development of imaging methods for chicken inspection has generally focused on methods to accentuate spectral and spatial features of carcasses, but not necessarily in connection to how these features are perceived through human vision. Color appearance models such as those ratified by the International Commission on Illumination (CIE) are often used in color imaging applications related to human color vision. Ding *et al.* (2005, 2006) investigated two-band color mixing for visual differentiation of the color appearance of several categories of chicken carcass condition, including wholesome, septicemia, and cadaver carcasses. Selection of waveband pairs to enhance differentiation between the categories was based on calculations of color difference and chromaticness difference indices from visible reflectance spectra of chicken samples. Simulation using the revised 1997 CIE color appearance model (CIECAM97) was performed to objectively evaluate the visual enhancement provided by an optical color-mixing device implementing the selected waveband pairs. It was found that single-category visual differentiation produced the best results when using pairs of filters, each 10 nm full width at half maximum (FWHM), as follows: 449 nm and 571 nm for wholesome carcasses, 454 nm and 590 nm for septicemia carcasses, and 458 nm and 576 nm for cadaver carcasses. Visually perceived

differences between all the categories of chicken conditions (i.e. multi-category differentiation) could be enhanced by an optical color-mixing tool using filters centered at 454 nm and 578 nm.

7.4.3. Target-triggered Multispectral Imaging Systems

Initial development of a multispectral imaging chicken inspection system involved a three-channel common-aperture camera to simultaneously acquire spatially-matched three-waveband image data. The multispectral imaging system consisted of the common aperture camera (MS2100, DuncanTech, Auburn, CA, USA), a frame grabber (PCI-1428, National Instruments, Austin, TX, USA), an industrial computer, and eight 100W tungsten–halogen lights (Yang *et al.*, 2005). A color-separating prism split broadband light entering the camera lens into three optical channels, each of which passed through an interference filter placed before a CCD imaging array. Control of the camera settings, such as triggering mode, output bit depth, and the integration time of exposure and the analog gain at the CCD sensor before the image was digitized for each imaging channel, was accomplished using the CameraLink utility program (DuncanTech, Auburn, CA, USA). Signals from the CCD imaging arrays were digitized by the frame grabber. An 8-bit image was saved from each of the three channels; the selection of interference filters for the three channels was based on the results of previous studies (Liu & Chen, 2000, 2001; Ding *et al.*, 2005). Commercially available interference filters with center wavelengths at 461.75 nm (20.78 nm FWHM), 541.80 nm (18.31 nm FWHM), and 700.07 nm (17.40 nm FWHM) were used for the three-channel common aperture camera. Image data acquisition was performed for 174 wholesome, 75 inflammatory process, and 170 septicemia chicken carcasses on a pilot-scale processing line in the laboratory operating at a speed of 70 bpm. It was found that despite individually adjustable settings for gain and integration times for the three channels, simultaneously obtaining high-quality images across all three channels was difficult owing to a variety of factors, such as avoiding both image saturation at 700 nm and inadequate image intensity at 460 nm, due to the spectral characteristics of the tungsten–halogen illumination (increasing intensity with increasing wavelengths) and CCD detector sensitivity (low sensitivity under 500 nm). Integration times were finally settled at 5 ms, 10 ms, and 18 ms for the 700 nm, 540 nm, and 460 nm channels, respectively. Off-line image processing algorithms based on PCA and selection of region of interest (ROI) were developed as inputs to a decision tree classification model. This model was able to classify 89.6% of wholesome,

94.4% of septicemia, and 92.3% of inflammatory process chicken carcasses (Yang *et al.*, 2005).

Another common-aperture multispectral chicken inspection system was developed for detection of tumors on chicken carcasses (Chao, Mehl *et al.*, 2002). An enclosed illumination chamber was used to acquire multispectral images of individual chicken carcasses by the three-channel prism-based common-aperture camera (TVC3, Optec, Milano, Italy). The prism assembly of the camera system separated full spectrum visible light into three broadband channels (red, green, and blue). An 8-bit image (728 × 572 pixels each) was produced by one CCD for each channel and captured by a frame grabber (XPG-1000, Dipix, Ontario, Canada). The three CCDs were each preceded by a replaceable narrow band filter. The perfect image registration resulting from the use of the three CCDs allowed for true multispectral images of subjects in the illumination chamber. AC regulated 150W quartz–halogen source illumination was delivered to the chamber by a pair of fiber-optic line lights.

Selection of filter wavelengths to use the three-CCD system for tumor detection was based on hyperspectral analysis using a laboratory bench-top hyperspectral imaging system (Lu & Chen, 1998; Kim *et al.*, 2001) developed in-house. This hyperspectral imaging system used a CCD camera system (SpectraVideo, PixelVision, OR, USA) equipped with an imaging spectrograph (SPECIM Inspector, Spectral Imaging, Oulu, Finland), to capture a series of hyperspectral line-scan images from a linear field of view across the width of a conveyor belt. Each hyperspectral line-scan image consisted of 402 spatial pixels (spanning the width of sample presentation on the conveyor belt) and 120 spectral pixels spanning 420–850 nm. Samples on a conveyor belt were illuminated with light from a pair of 21V, 150W halogen lamps powered with a regulated DC voltage power supply (Fiber-Lite A-240P, Dolan-Jenner Industries, MA, USA). Eight chicken carcasses were placed on the conveyor belt, one at a time, and moved across the linear field of view while a series of line-scan images were acquired. These line-scan images were then compiled to form a complete hyperspectral image for each chicken carcass. Spatial ROIs from the hyperspectral images of eight chicken carcasses, each exhibiting tumors, were selected to include tumor areas and some surrounding normal skin tissue around the tumors. ENVI 3.2 software (Research Systems, Inc., CO, USA) was used to perform PCA. The principal component images for the tumor ROIs were visually examined to select the principal component showing the greatest contrast between tumor areas and normal skin. Identification of filters for multispectral detection of tumors was based on analysis for the major wavelengths contributing to the principal

component producing the greatest visual contrast between tumors and normal skin on the chicken carcasses.

Two significant visible wavebands were noted from the weighted wavelength distribution corresponding to the eigenvector defined on chicken skin tumors that provided the best contrast between tumors and normal chicken skin: 475 nm and 575 nm. These wavebands correspond to metmyoglobin and oxymyoglobin bands (Liu & Chen, 2000). Because the far red region was previously found to be insensitive to surface defects on chickens (Park & Chen, 1994), bands in this region could therefore be utilized for masking and normalization of chicken carcass images. A filter centered at 705 ± 10 nm was chosen for this purpose, to be used with filters at 465 ± 10 nm and 575 ± 10 nm for the adaptable three-band CCD camera (the ± 10 nm designates the FWHM bandpass). Feature extraction from the variability of ratioed multispectral images, including mean, standard deviation, skewness, and kurtosis, provided the basis for fuzzy logic classifiers, which were able to separate normal from tumorous skin areas with increasing accuracies as more features were used. In particular, use of all three features gave successful detection rates of 91% and 86% for normal and tumorous tissue, respectively.

A high-resolution single-CCD imaging system utilized with an optical adaptor was also investigated for multispectral imaging inspection of wholesome vs. systemically diseased chicken carcasses (Yang *et al.*, 2006). This multispectral imaging system consisted of an image splitter (MultiSpec Imager, Optical Insights, LLC, Santa Fe, NM, USA), a back-illuminated CCD camera (SpectraVideo SV 512, PixelVision, Inc., Tigard, OR, USA), a PMB-004 shutter and cooler control board, a PMB-007 serial interface board, a PMJ-002 PCI bus data acquisition board, a LynxPCI frame grabber, a computer, and four 100W tungsten halogen lights. Four interference filters and an optical mirror assembly were used to create four waveband images of the target that were acquired simultaneously on a single CCD focal plane. The resulting 16-bit multispectral image contained four sub-images. The PixelView version 3.20 utility program (PixelVision, Inc., Tigard, OR, USA) was used to control camera settings, such as integration time and image acquisition.

Multispectral ROI features were developed to differentiate wholesome and systemically diseased chickens. Due to significant color differences between wholesome and systemically diseased chickens at 488 nm, 540 nm, and 580 nm, interference filters were selected at these wavebands for the multispectral imaging system; one additional filter was selected at 610 nm for image masking purposes. An algorithm was developed to find the ROI on the multispectral images. Classification thresholds for identifying wholesome and systemically diseased chickens were determined using

a Classification and Regression Tree (CART) decision tree algorithm for 48 features per image that were defined by a combination of waveband, feature type, and classification area.

Multispectral images of a selected ROI for 332 wholesome and 328 systemic diseased chickens, using wavelengths at 488 nm, 540 nm, 580 nm, and 610 nm, were collected for image processing and analysis. The 610 nm image was used to create a mask to extract chicken images from background. Using a decision tree model, classification accuracies of 96.3% and 98.6% for wholesome and systemic diseased carcasses, respectively, were achieved.

7.5. DEVELOPMENT OF LINE-SCAN IMAGING FOR ON-LINE POULTRY INSPECTION

Although hyperspectral line-scan imaging was first used as a laboratory tool to develop target-triggered multispectral imaging systems, several key technological advances enabled the development of hyperspectral line-scan imaging for direct implementation in high-speed on-line inspection systems. In particular, the implementation of Electron-Multiplying Charge-Coupled-Device (EMCCD) detectors in camera systems and their use with imaging spectrographs made possible high-speed line-scan imaging systems capable of both hyperspectral and multispectral on-line imaging at the high speeds required by commercial poultry processing lines. As a result, both hyperspectral analysis for method development and multispectral implementation could be performed using the same on-line line-scan imaging system, greatly facilitating both method development and implementation.

7.5.1. Spectral Line-Scan Imaging System

Conventional development of multispectral inspection methods for on-line applications involves determination of specific spectral parameters using a hyperspectral imaging system or spectroscopy-based methods, followed by subsequent implementation of the parameters for use in a separate multispectral imaging system. The conversion and implementation of parameters from one system to another usually requires time-consuming cross-system calibration. The capability of a single system to operate in either hyperspectral or multispectral imaging mode can eliminate the need for cross-system calibration and ensure higher accuracy performance. This single-system approach was taken in the development of a line-scan imaging system capable of operating in either hyperspectral or multispectral imaging mode on a chicken processing line.

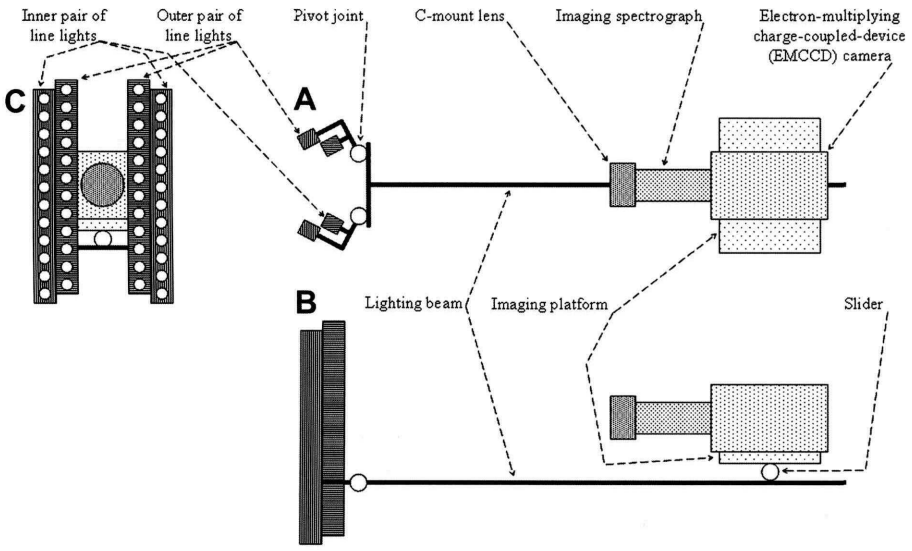

FIGURE 7.3
Schematic of the hyperspectral/multispectral line-scan imaging system in (A) overhead view, (B) side view, and (C) front view

Figure 7.3 shows the components of the hyperspectral/multispectral line-scan imaging system, including an EMCCD camera, an imaging spectrograph, a C-mount lens, and two pairs of high power, broad-spectrum white light emitting diode (LED) line lights. The EMCCD camera (PhotonMAX 512b, Roper Scientific, Inc., Trenton, NJ, USA) has 512 × 512 pixels and is thermoelectrically cooled to approximately −70 °C (via a three-stage Peltier device). An imaging spectrograph (ImSpector V10OEM, Specim/Spectral Imaging Ltd., Oulu, Finland), and a C-mount lens (Rainbow CCTV S6x11, International Space Optics, S.A., Irvine, CA, USA) are attached to the EMCCD imaging device. The 50 μm aperture slit of the spectrograph limits the instantaneous field of view (IFOV) of the imaging system to a thin line for line-scan imaging. Light from the IFOV is dispersed by a prism–grating–prism line-scan spectrograph and projected onto the EMCCD imaging device. The spectrograph creates a two-dimensional (spatial and spectral) image for each line-scan, with the spatial dimension along the horizontal axis and the spectral dimension along the vertical axis of the EMCCD imaging device. Thus, for hyperspectral imaging, a full spectrum is acquired for every pixel in each line scan (Figure 7.4). The spectral distribution of useful wavelengths and the size of the spatial image features to be processed determine the parameters for image binning, which reduces the number of image pixels and increases the signal-to-noise ratio by adding together photons from adjacent pixels in the detector array. More specific selection of wavelengths, spatial image size, and associated parameters such as binning can be optimized for

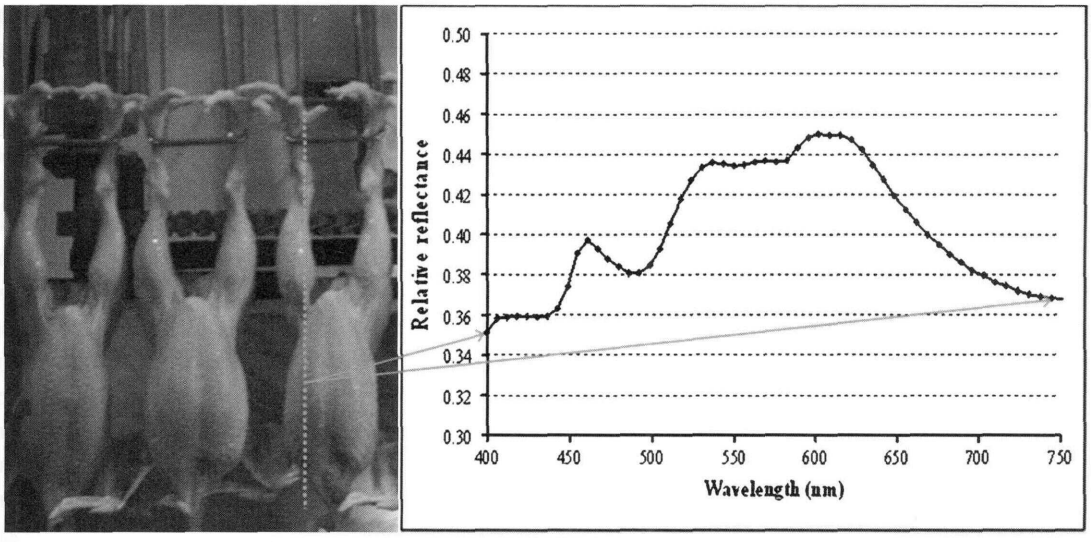

FIGURE 7.4 *Full-spectrum data is acquired for every pixel in each hyperspectral line-scan image. (Full color version available on http://www.elsevierdirect.com/companions/9780123747532/)*

either hyperspectral or multispectral imaging—for high-speed chicken processing, the capacity for short-exposure low-light imaging provided by the EMCCD detector is vital to successful on-line use in either mode. Pixels from the detector are binned by the high-speed shift register (which is built into the camera hardware) and transferred to the 16-bit digitizer, which has a rapid pixel-readout rate of approximately 10 MHz. The digitizer performs rapid analog-to-digital conversion of the image data for each line-scan image. The rapid image acquisition is followed by computer image analysis for real-time classification of wholesome and unwholesome pixels in the line-scan images of the chicken carcasses.

7.5.2. Hyperspectral Imaging Analysis

In hyperspectral imaging mode, a 55-band spectrum was acquired for each of the 512 spatial pixels in every hyperspectral line-scan image. The original hyperspectral line-scan image size (512 × 512 pixels) was reduced by 1 × 4 binning to produce line-scan images with a spectral resolution of 128 pixels (512 divided by 4) in the spectral dimension. Because the useful spectrum of light from the LED illumination did not span the entire width of the EMCCD detector, the first 20 and last 53 spectral bands were discarded, resulting in a final hyperspectral line-scan image size of 512 × 55 pixels. Hyperspectral images of wholesome and systemically diseased chickens, compiled from

line-scans acquired on a 140 bpm commercial processing line, were analyzed off-line using MATLAB software (MathWorks, Natick, MA, USA) to determine ROI and spectral waveband parameters for use in multispectral wholesomeness inspection of the chickens.

For analysis, the 620 nm waveband was selected for masking purposes to remove the image background using a 0.1 relative reflectance threshold value. For any pixel in a hyperspectral line-scan, if its reflectance at 620 nm was below the threshold value, then that pixel was identified as background and its value at all wavebands was re-assigned to zero. The background-removed line-scan images were compiled to form images of chicken carcasses for a set of wholesome birds and a set of unwholesome birds. These images were analyzed to determine the parameters for an optimized ROI for use in differentiating wholesome and unwholesome birds. Within each bird image (Figure 7.5), the potential ROI area spanned an area from an upper border across the body of the bird to a lower border at the lowest non-background spatial pixel in each line scan, or to the last (512th) spatial pixel of the line-scan if there were no background pixels present at the lower edge. For each potential ROI, the average relative reflectance spectrum was calculated across all ROI pixels from all wholesome chicken images, and the average relative reflectance spectrum was also calculated across all ROI pixels from all unwholesome chicken images. The difference spectrum between the wholesome and unwholesome average spectra was calculated. This calculation was performed for all potential ROIs evaluated, which varied in size and

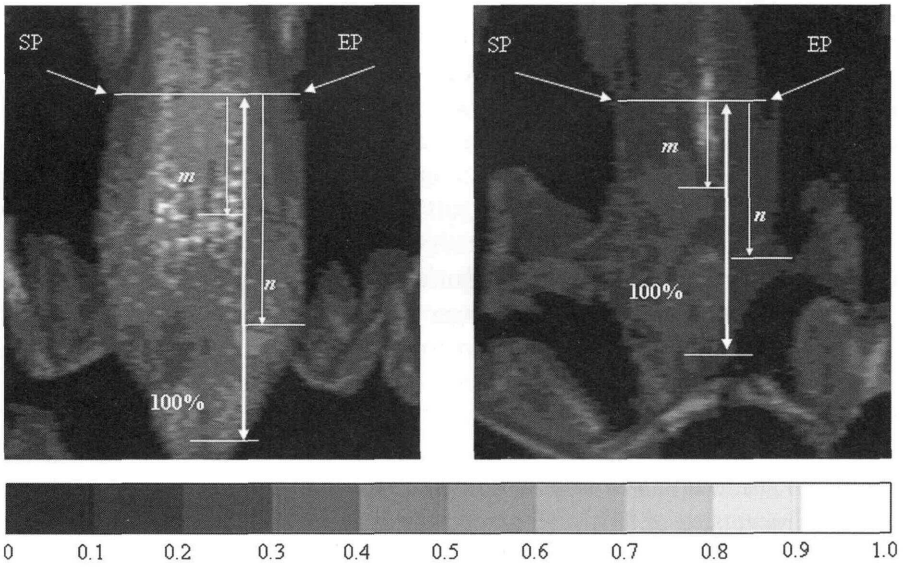

FIGURE 7.5

Contour images of two chicken carcasses marked with example locations of the SP, EP, m, and n parameters used for locating the ROI

were defined by the number of ROI pixels and their vertical coordinate locations within each line-scan. The optimized ROI was identified as the one that provided the greatest spectral difference between averaged wholesome pixels and averaged unwholesome pixels across all 55 wavebands.

A contour image of two example birds is shown in Figure 7.5, with the Starting Point and Ending Point (SP and EP, respectively) marked on each. Within each line-scan, possible ROI pixels begin at the SP–EP line and extend to the furthest non-background pixel below the SP–EP line, which in some cases coincides with the pixel at the far edge of the line-scan image. Parameters m and n indicate, as percentages of the pixel length between the SP–EP line and the furthest non-background pixel within each line-scan image, the location of the upper and lower ROI boundaries for ROIs under consideration. To optimize the ROI size and location, combinations of m and n were evaluated with values of m between 10% and 40% and values of n between 60% and 90%. For each possible ROI, the average spectrum was calculated across all ROI pixels from the 5 549 wholesome chicken carcasses, and the average spectrum was calculated across all ROI pixels from the 93 unwholesome chicken carcasses. The difference between the average wholesome and average unwholesome value at each of the 55 wavebands was calculated. Figure 7.6 shows the range of these 55 values for each possible ROI. Across all the possible ROIs, wavebands near 580 nm showed the

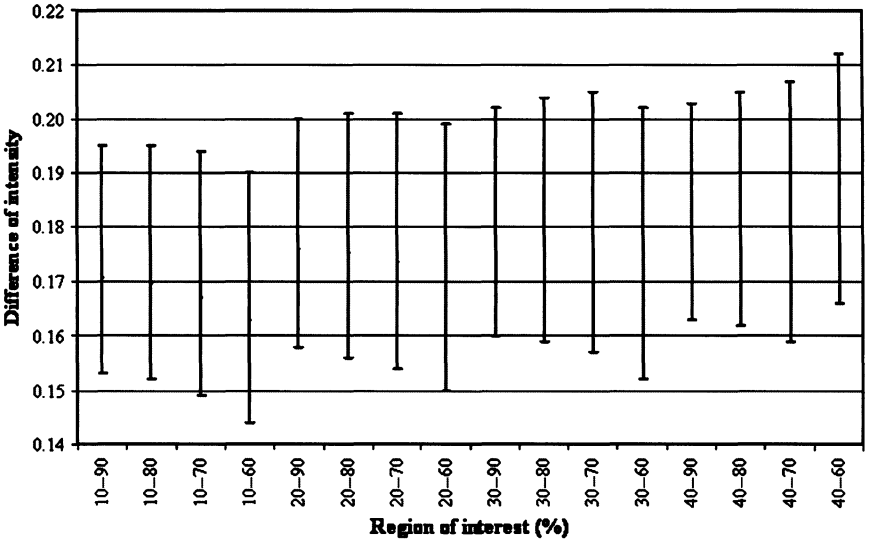

FIGURE 7.6 *Plot of the range of difference values between average wholesome and average unwholesome chicken spectra for ROIs evaluated during hyperspectral analysis to optimize the ROI selection for multispectral inspection of chickens*

highest difference between the average wholesome and average unwholesome spectra, and wavebands near 400 nm showed the lowest difference values. The 40–60% ROI showed the highest difference values overall, with the highest value of 0.212 occurring at 580 nm, and was thus the final ROI selection.

Using the optimized ROI, a single waveband was identified as being the waveband corresponding to the greatest spectral difference between averaged wholesome chicken pixels and averaged unwholesome chicken pixels, for differentiating wholesome and unwholesome chicken carcasses by relative reflectance intensity. The average wholesome and average unwholesome spectra from the optimized ROI were also examined for wavebands at which local maxima and minima occurred, to identify wavebands that might be used in two-waveband ratios for differentiating wholesome and unwholesome birds. The value of each potential band ratio was calculated for the average wholesome chicken pixels and for the average unwholesome chicken pixels. The two-waveband ratio showing the greatest difference in ratio value between average wholesome and average unwholesome chicken pixels was selected.

Figure 7.7 shows the average spectra for pixels within this optimized ROI from all line-scan images in the wholesome data set and in the unwholesome

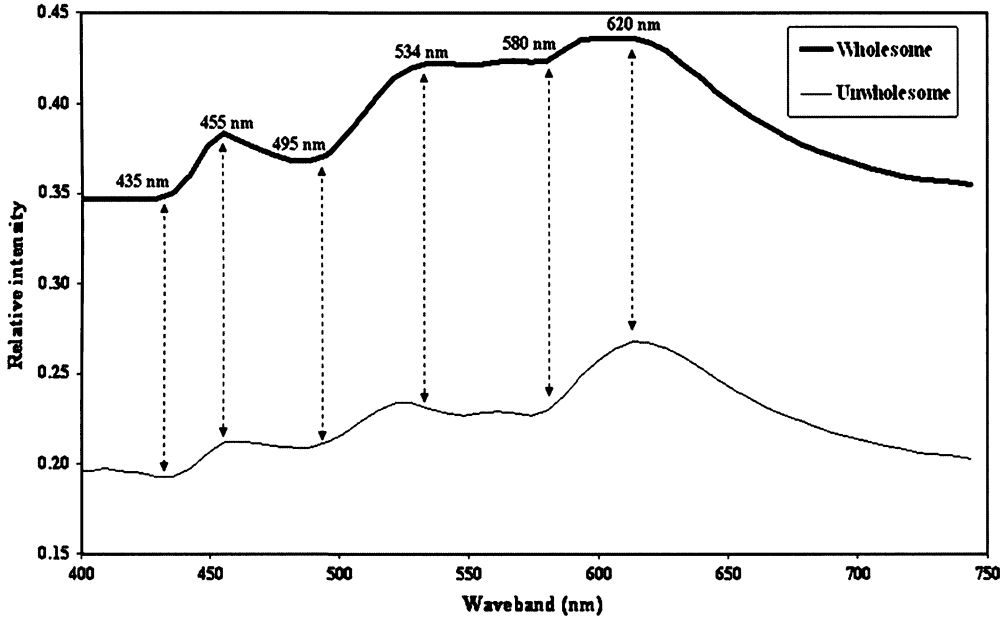

FIGURE 7.7 *The average ROI pixel spectrum for wholesome chickens and the average ROI pixel spectrum for unwholesome chickens, used to select wavebands for intensity- and ratio-based differentiation*

data set. Because the 580 nm band showed the greatest difference between the average wholesome and the average unwholesome spectra, this band was selected as the single waveband to be used for intensity-based differentiation of wholesome and unwholesome chicken carcasses. Six possible wavebands (also marked on Figure 7.7) were investigated for differentiation of wholesome and unwholesome chicken carcasses by a two-waveband ratio. Because visual examination showed noticeable differences between the average wholesome and average unwholesome spectral slopes in the three areas corresponding to 440–460 nm, 500–540 nm, and 580–620 nm, two-band ratios were investigated using these particular pairings. Two-band ratios for these pairings were calculated using the average wholesome reflectance, W, and average unwholesome reflectance, U, values. The differences in ratio value between wholesome and unwholesome were then calculated:

$$W_{440}/W_{460} - U_{440}/U_{460} = 0.003461$$

$$W_{500}/W_{540} - U_{500}/U_{540} = 0.038602$$

$$W_{580}/W_{620} - U_{580}/U_{620} = 0.115535$$

The last ratio, using the 580 nm and 620 nm wavebands, showed the greatest difference between the average wholesome and average unwholesome chicken spectra and was thus selected for use in differentiation by two-waveband ratio.

7.5.3. On-Line Multispectral Inspection

After hyperspectral analysis to select specific wavebands for multispectral inspection of chicken carcasses, the same line-scan imaging system was operated in multispectral imaging mode to use those selected wavebands for real-time inspection. Thus, there remained 512 pixels in the spatial dimension of the image but the pixels in the spectral dimension were further reduced from 55 to only two wavebands, with the elimination of unnecessary waveband data enabling even faster imaging speed. The ability of the spectral line-scan imaging system's EMCCD camera to use a very short integration time (0.1 ms) with a high gain setting, along with the selection of a limited number of pixels in the spectral dimension of the line-scan images, were vital to the system's successful on-line operation in multispectral imaging mode for differentiating wholesome and systemically diseased chickens at 140 bpm.

The capability to detect individual bird carcasses, classify the carcass condition, and generate a corresponding output useful for process control, all

at speeds compatible with on-line operations, is required for effective multispectral imaging inspection for wholesomeness of chicken carcasses on a commercial processing line. LabVIEW 8.0 (National Instruments Corp., Austin, TX, USA) software was used to develop in-house inspection modules to control the spectral imaging system for performing these tasks in real-time. The following algorithm, based on the imaging system's line-by-line mode of operation, was developed to detect the entry of a bird carcass into the IFOV and classify the carcass as either wholesome or unwholesome using real-time multispectral inspection on a processing line.

Figure 7.8 shows a flowchart describing the line-by-line algorithm for multispectral inspection. First, a line-scan image was acquired that contained only raw reflectance values at the two key wavebands needed for intensity and ratio differentiation; these raw reflectance data were converted into relative reflectance data and background pixels were removed from the image (Figure 7.8, Box 8.1). The line-scan image was checked for the presence of the SP of a new bird (Figure 7.8, Box 8.2); if no SP was present, no further analysis was performed for this line-scan image and a new line-scan image was acquired. If the line-scan was found to contain an SP, then the ROI pixels were located (Figure 7.8, Box 8.3) and the decision output value of D_o was calculated for each ROI pixel in the line-scan image (Figure 7.8, Box 8.4), before a new line-scan image was acquired. With each new line-scan image acquired (Figure 7.8, Box 8.5), the ROI pixels were located, and the decision output value of D_o was calculated for each pixel, until the EP of that bird was detected (Figure 7.8, Box 8.6), indicating no additional line-scan images to be analyzed for that carcass. The average D_o value for the bird was calculated across all its ROI pixels (Figure 7.8, Box 8.9) and then compared to the threshold value (Figure 7.8, Box 8.10) for the final determination of wholesomeness or unwholesomeness for the bird carcass (Figure 7.8, Boxes 8.11 and 8.12). The decision output D_o calculation was based on fuzzy inference classifiers (Chao *et al.*, 2008) developed using mean and standard deviation values for ROI reflectance at the key wavebands during hyperspectral analysis of the wholesome and unwholesome sets of chicken images.

7.5.4. In-Plant Evaluation

Hyperspectral line-scan images of chickens were first acquired on a 140 bpm commercial chicken processing line for a total of 5 549 wholesome and 93 unwholesome chickens, with their conditions identified by an FSIS veterinary medical officer who observed the birds as they approached the illuminated IFOV of the imaging system. The 55-band hyperspectral data for the chicken carcasses were analyzed as described in Section 7.5.2 for ROI

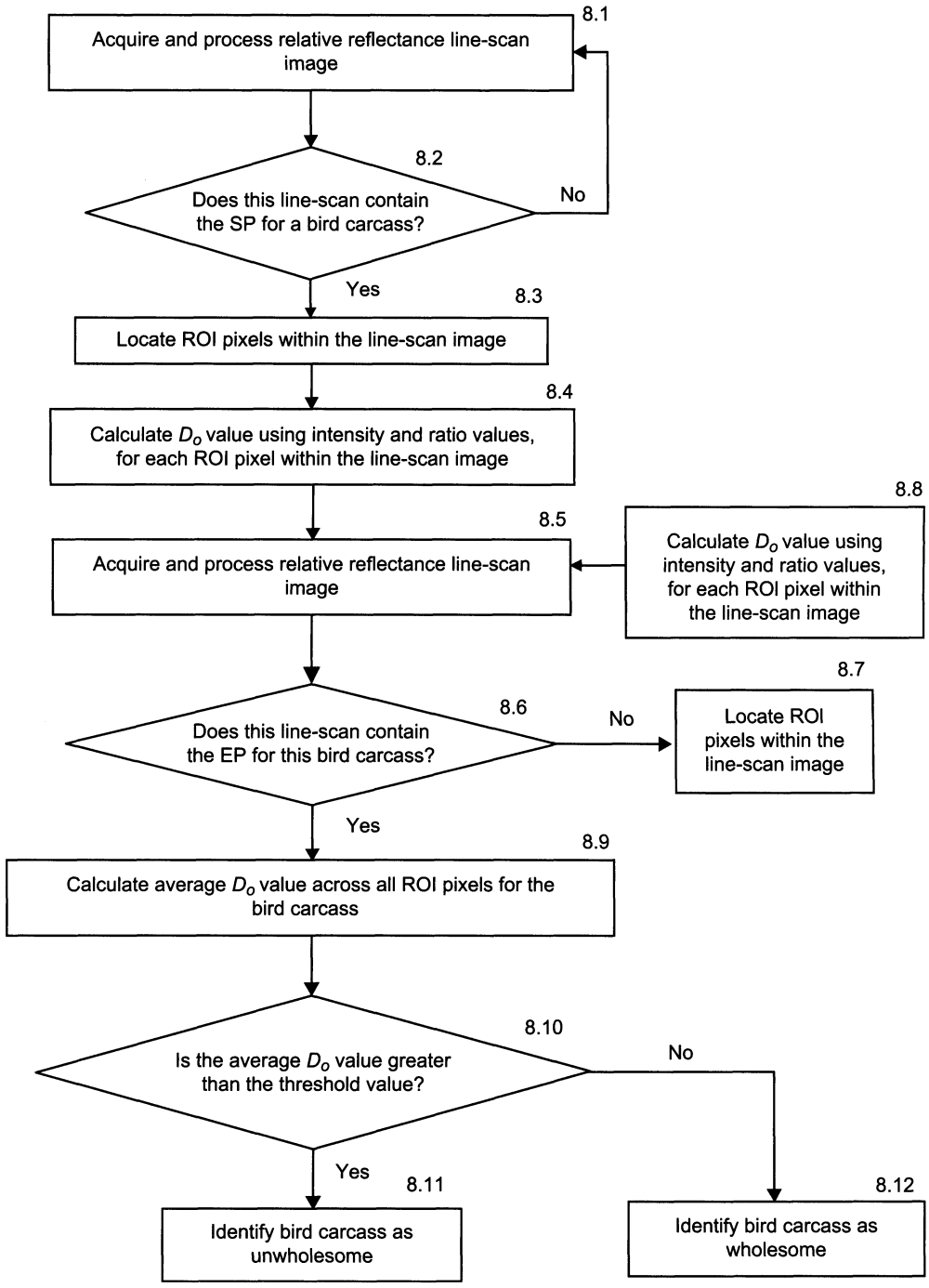

FIGURE 7.8 *A flowchart of the line-by-line algorithm for on-line multispectral wholesomeness inspection by the spectral line-scan imaging system*

optimization and for selection of one key wavelength and one two-waveband ratio, based on average spectral differences between wholesome and unwholesome birds. Multispectral imaging for on-line high-speed inspection in real time used only the two selected wavelengths for intensity- and ratio-based differentiation. LabView-based software modules were developed for detecting each bird and for implementing the on-line inspection algorithms. On-line multispectral inspection was tested on a commercial processing line over two 8-hour shifts during which over 100 000 birds were inspected by the imaging system. To verify system performance, an FSIS veterinary medical officer identified wholesome and unwholesome conditions of birds immediately before they entered the IFOV of the imaging system, during several 30–40 minute periods, for direct comparison with the classification results produced by the multispectral imaging system.

Figure 7.9 shows examples of chicken images acquired on-line, with the ROI pixels highlighted on each bird. During on-line operation, the inspection program automatically located the 40–60% ROI with the acquisition of each line-scan image. As shown, the ROI location was clearly affected by the size and position of the bird and thus varied between different birds. For a bird whose body extended past the lower edge of the image, such as the first bird in Figure 7.9, the ROI encompassed a rectangular area. In contrast, an irregularly shaped ROI resulted for birds positioned such that background pixels were present at the lower edge of the image.

The first image in Figure 7.10 (*top*) shows a masked image of nine chickens, highlighting all the ROI pixels for each bird. Using fuzzy inference classifiers (Chao *et al.*, 2007), two D_o values were calculated (ranging between 0 and 1) for each pixel in the ROI, one for the key waveband and one for the two-waveband ratio. On-line multispectral inspection averaged the D_o values for all ROI pixels for each bird, in order to classify the bird by comparison to the threshold value of 0.6. For illustration purposes, the second image in Figure 7.10 (*bottom*) highlights the results of classifying the individual pixels in the ROIs (instead of classifying whole birds), obtained by

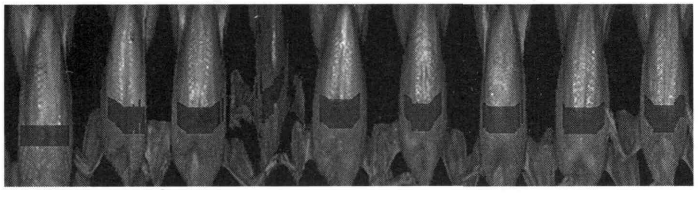

FIGURE 7.9 *Automated ROI identification highlighted on the images of nine chicken carcasses. (Full color version available on http://www.elsevierdirect.com/companions/9780123747532/)*

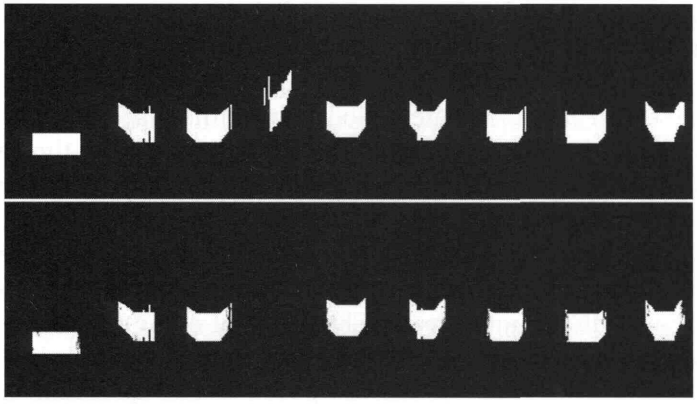

FIGURE 7.10 *A masked image (top) of nine chickens that highlights the ROI pixels to be analyzed for each chicken, and a second image (bottom) highlighting individual pixels within each ROI that were classified as wholesome*

averaging the two D_o values for each ROI pixel in the top image and comparing the average value with the 0.6 threshold value. In this illustrative example, the fourth chicken from the left is an unwholesome bird and all of its ROI pixels were individually identified as unwholesome, consequently not appearing at all in the second image.

Table 7.1 shows the total counts of chickens identified by the imaging system as being either wholesome or unwholesome during the two 8-hour shifts of on-line multispectral inspection. Numbers drawn from FSIS tally sheets, created by three inspection stations on the same processing line during the same inspection shifts, are shown for comparison. Although direct bird-to-bird comparison between the imaging inspection system and the inspectors was not feasible, the percentages indicate that the relative numbers of wholesome and unwholesome birds identified by the imaging

Table 7.1 Counts of wholesome and unwholesome birds identified on the processing line during inspection shifts by human inspectors and by the hyperspectral/multispectral line-scan imaging inspection system

	Line inspectors			Imaging inspection system		
Shift	**Wholesome**	**Unwholesome**	**Total**	**Wholesome**	**Unwholesome**	**Total**
1	53563 (99.84%)	84 (0.16%)	53647 (100%)	45305 (99.37%)	288 (0.63%)	45593 (100%)
2	64972 (99.89%)	71 (0.11%)	65043 (100%)	60922 (99.84%)	98 (0.16%)	61020 (100%)

inspection system and by the processing line inspectors were not significantly different.

System verification was also performed by an FSIS veterinary medical officer for several 30–40 minute periods within the inspection shifts. This consisted of bird-by-bird observation of chicken carcasses on the processing line immediately before they entered the IFOV of the imaging system; the imaging system output was compared with the veterinary medical officer's identifications. Over four verification periods during inspection shift 1, the imaging system correctly identified 99.3% of wholesome birds (16 056 of 16 174) and 95.4% of unwholesome birds (41 of 43). Over six verification periods during inspection shift 2, the imaging system correctly identified 99.8% of wholesome birds (27 580 of 27 626) and 97.1% of unwholesome birds (34 of 35). These verification period results, together with the whole-shift comparison results against tally sheets (Table 7.1), demonstrate that the hyperspectral/multispectral line-scan imaging inspection system can perform effectively on a 140 bpm high-speed commercial poultry processing line.

7.5.5. Commercial Applications

This work successfully demonstrates the potential of a hyperspectral/multispectral line-scan imaging system for effective on-line inspection of chickens. The spectral resolution of the imaging system was approximately 7 nm (FWHM). On the 140 bpm processing line, the imaging system was able to acquire approximately 50 hyperspectral (55-waveband) line-scan images per bird, for a spatial resolution of 0.35 mm in the hyperspectral images that were analyzed for waveband selection, with the ROI of any given bird spanning approximately 20–30 of those 50 line-scan images. During multispectral on-line inspection, the ROI per bird spanned approximately 40 multispectral (2-waveband) line-scan images, depending on the bird size. With about 4 000 pixels in the ROI to analyze for multispectral classification of a bird, the spatial resolution of the system is more than adequate for accurate and effective detection of unwholesome chickens at a speed of 140 bpm.

Automated on-line pre-sorting of broilers is an ideal application for this spectral line-scan imaging system. By detecting and diverting unwholesome birds exhibiting symptoms of systemic disease earlier on the processing line, production and efficiency can be improved—fewer unwholesome birds will be presented for inspection by human inspectors and fewer empty shackles (nearer 100% operating capacity) will occur during downstream processing. By diverting most unwholesome birds earlier, the reduced inspection

workload for human inspectors can provide the opportunity for inspectors to address additional tasks beyond direct carcass inspection. The rejected birds are detected and diverted while still on the high-speed kill line, prior to automatic re-hanging on the evisceration line, which helps to reduce food safety risks from possible cross-contamination. For the small number of wholesome birds that might be misidentified as false positives by the automated inspection system, a processing plant can opt to re-inspect diverted birds and manually transfer any wholesome birds to the evisceration line.

For the purpose of pre-sorting young chickens on commercial processing lines, the spectral line-scan imaging technology has been recently reviewed and approved by the USDA FSIS Risk and Innovations Management Division. Commercialization of this system for industrial use will be the first application of spectral line-scan imaging technology for a food safety inspection task.

7.6. CONCLUSIONS

Due to increasing production needs and food safety concerns facing the poultry industry in the United States and worldwide, automated systems developed for safety inspection of poultry products on high-speed processing lines will be essential in the future. By enabling poultry producers and regulatory agencies to satisfy high-throughput production and inspection requirements more efficiently, science-based automated food inspection systems can help alleviate the pressures on human inspectors, improve production throughput, and grow public confidence in the safety and quality of the food production and distribution system. Development of automated non-destructive food safety inspection methods based on spectroscopy and spectral imaging have been one of the major ARS research priorities over the last decade.

VIS/NIR spectroscopy methods were first developed and demonstrated capable of over 90% accuracies on high-speed processing lines in differentiating wholesome chickens from unwholesome birds exhibiting systemic conditions; however, given the lack of spatial information, the field of application for VIS/NIR spectroscopy inspection systems was considered limited. In this light, expansion of the spectral techniques to multispectral imaging was sought, requiring investigation and development of wavelength selection methods such as 2-D spectral correlation, color mixing, and hyperspectral imaging analysis—with the addition of spatial information for whole bird carcasses, such wavelength selection was necessary to reduce image data volumes for practical application. Dual-camera and common-aperture

systems for target-based multispectral imaging were developed, but encountered some problems with short-exposure image acquisition and processing speed during implementation on commercial processing lines.

Hyperspectral imaging was first used for spectral analysis to select wavelengths for implementation in automated multispectral imaging systems, and in itself was effective for laboratory-based research. The introduction of EMCCD cameras and their use with imaging spectrographs was a key development that enabled automated line-scan spectral imaging at the high speeds found on commercial processing lines, and was particularly important for allowing a single imaging system to perform both hyperspectral and multispectral imaging. With the transition from target-based imaging to line-scan imaging, algorithms such as line-scan target detection were a necessary development for effective on-line implementation. Not only could such algorithms streamline or simplify the processing-line imaging operations, for example by eliminating sensors formerly needed to trigger accurate imaging of individual birds on the line, but they also provided potential value-added applications that could be performed using the same image data—for example, quality inspection tasks such as assessing defects, size, shape, or weight attributes. The results of in-plant testing showed that the ARS line-scan spectral imaging system could successfully inspect chickens on high-speed processing lines operating at 140 bpm, accurately differentiating between wholesome and unwholesome birds. The system can be used for on-line pre-sorting of birds on commercial poultry processing lines, thereby increasing efficiency, reducing labor and costs, and producing significant benefits for poultry producers and processors.

NOMENCLATURE

2-D correlation	two-dimensional spectral correlation
ARS	Agricultural Research Service
bpm	birds per minute
CART	classification and regression tree
CCD	charge-coupled device
CIE	International Commission on Illumination
CIECAM	CIE color appearance model
EMCCD	electron-multiplying charge-coupled device
EP	ending point
FSIS	Food Safety and Inspection Service
FWHM	full width at half maximum

HACCP	Hazard Analysis and Critical Control Point
HIMP	HACCP-Based Inspection Models Project
IFOV	instantaneous field of view
IP	inflammatory process
LED	light emitting diode
NELS	New Line Speed
PCA	principal component analysis
PDA	photodiode array
PPIA	Poultry Product Inspection Act
ROI	region of interest
septox	septicemia/toxemia
SIS	Streamlined Inspection System
SP	starting point
USDA	United States Department of Agriculture
VIS/NIR	visible/near-infrared

REFERENCES

Chao, K., Chen, Y. R., Early, H., & Park, B. (1999). Color image classification system for poultry viscera inspection. *Applied Engineering in Agriculture, 15*(4), 363–369.

Chao, K., Park, B., Chen, Y. R., Hruschka, W. R., & Wheaton, F. W. (2000). Design of a dual-camera system for poultry carcasses inspection. *Applied Engineering in Agriculture, 16*(5), 581–587.

Chao, K., Mehl, P. M., & Chen, Y. R. (2002). Use of hyper- and multi-spectral imaging for detection of chicken skin tumors. *Applied Engineering in Agriculture, 18*(1), 78–84.

Chao, K., Chen, Y. R., Hruschka, W. R., & Gwozdz, F. B. (2002). On-line inspection of poultry carcasses by a dual-camera system. *Journal of Food Engineering, 51*(3), 185–192.

Chao, K., Chen, Y. R., & Chan, D. E. (2003). Analysis of VIS/NIR spectral variations of wholesome, septicemia, and cadaver chicken samples. *Applied Engineering in Agriculture, 19*(4), 453–458.

Chao, K., Chen, Y. R., & Chan, D. E. (2004). A spectroscopic system for high-speed inspection of poultry carcasses. *Applied Engineering in Agriculture, 20*(5), 683–690.

Chao, K., Yang, C. C., Chen, Y. R., Kim, M. S., & Chan, D. E. (2007). Hyperspectral/multispectral line-scan imaging system for automated poultry carcass inspection applications for food safety. *Poultry Science, 86*, 2450–2460.

Chao, K., Yang, C. C., Kim, M. S., & Chan, D. E. (2008). High throughput spectral imaging system for wholesomeness inspection of chicken. *Applied Engineering in Agriculture, 24*(4), 475–485.

Chen, Y. R., & Massie, D. R. (1993). Visible/near-infrared reflectance and interactance spectroscopy for detection of abnormal poultry carcasses. *Transactions of the ASAE, 36*, 863–869.

Chen, Y. R., Huffman, R. W., Park, B., & Nguyen, M. (1995). A transportable spectrophotometer system for online classification of poultry carcasses. *Journal of Applied Spectroscopy, 50*(7), 910–916.

Chen, Y. R., Nguyen, M., & Park, B. (1998). Neural network with principal component analysis for poultry carcass classification. *Journal of Food Process Engineering, 21*, 351–367.

Chen, Y. R., Park, B., Huffman, R. W., & Nguyen, M. (1998). Classification of online poultry carcasses with back-propagation neural networks. *Journal of Food Process Engineering, 21*, 33–48.

Chen, Y. R., Hruschka, W. R., & Early, H. (2000). On-line trials of a chicken carcass inspection system using visible/near-infrared reflectance. *Journal of Food Process Engineering, 23*, 89–99.

Chen, Y. R., Chao, K., & Kim, M. S. (2002). Machine vision technology for agricultural applications. *Computers and Electronics in Agriculture, 36*, 173–191.

Ding, F., Chen, Y. R., & Chao, K. (2005). Two-waveband color-mixing binoculars for the detection of wholesome and unwholesome chicken carcasses: a simulation. *Applied Optics, 44*(26), 5454–5462.

Ding, F., Chen, Y. R., & Chao, K. (2006). Two-color mixing for classifying agricultural products for food safety and quality. *Applied Optics, 45*(4), 668–677.

Gowen, A. A., O'Donnell, C. P., Cullen, P. J., Downey, G., & Frias, J. M. (2007). Hyperspectral imaging—an emerging process analytical tool for food quality and safety control. *Trends in Food Science & Technology, 18*(12), 590–598.

Kim, M. S., Chen, Y. R., & Mehl, P. M. (2001). Hyperspectral reflectance and fluorescence imaging system for food quality and safety. *Transactions of the ASAE, 44*(3), 721–729, 2001.

Kim, M. S., Lefcourt, A. M., Chen, Y. R., Kim, I., Chan, D. E., & Chao, K. (2002). Multispectral detection of fecal contamination on apples based on hyperspectral imagery. Part II: Application of hyperspectral fluorescence imaging. *Transactions of the ASAE, 45*(6), 2039–2047.

Kim, M. S., Lefcourt, A. M., Chen, Y. R., & Kang, S. (2004). Hyperspectral and multispectral laser induced fluorescence imaging techniques for food safety inspection. *Key Engineering Materials, 270*, 1055–1063.

Lawrence, K. C., Park, B., Windham, W. R., & Mayo, C. (2003). Calibration of a pushbroom hyperspectral imaging system for agricultural inspection. *Transactions of the ASAE, 46*(2), 513–521.

Lawrence, K. C., Windham, W. R., Park, B., & Buhr, R. J. (2003). A Hyperspectral imaging system for identification of fecal and ingesta contamination on poultry carcasses. *Journal of Near-Infrared Spectroscopy, 11*(4), 269–281.

Liu, Y., & Chen, Y. R. (2000). Two-dimensional correlation spectroscopy study of visible and near-infrared spectral variations of chicken meats in cold storage. *Applied Spectroscopy, 54*(10), 1458–1470.

Liu, Y., & Chen, Y. R. (2001). Two-dimensional visible/near-infrared correlation spectroscopy study of thawing behavior of frozen chicken meats without exposure to air. *Meat Science, 57*(3), 299–310.

Lu, R., & Chen, Y. R. (1998). Hyperspectral imaging for safety inspection of foods and agricultural products. In Y. R. Chen (Ed.), *Pathogen detection and remediation for safe eating* (pp. 121–133). Bellingham, MA: SPIE—The International Society for Optical Engineering.

Lu, R., & Peng, Y. (2006). Hyperspectral scattering for assessing peach fruit firmness. *Biosystems Engineering, 93*(2), 161–171.

Mehl, P. M., Chao, K., Kim, M. S., & Chen, Y. R. (2002). Detection of defects on selected apple cultivars using hyperspectral and multispectral image analysis. *Applied Engineering in Agriculture, 18*(2), 219–226.

Noh, H., & Lu, R. (2007). Hyperspectral laser-induced fluorescence imaging for assessing apple quality. *Postharvest Biology and Technology, 43*(2), 193–201.

Park, B., & Chen, Y. R. (1994). Intensified multi-spectral imaging system for poultry carcass inspection. *Transactions of the ASAE, 37*, 1983–1988.

Park, B., & Chen, Y. R. (1996). Multispectral image co-occurrence matrix analysis for poultry carcass inspection. *Transactions of the ASAE, 39*(4), 1485–1491.

Park, B., & Chen, Y. R. (2000). Real-time dual-wavelength image processing for poultry safety inspection. *Journal of Food Process Engineering, 23*(5), 329–351.

Park, B., Lawrence, K. C., Windham, W. R., & Buhr, R. J. (2002). Hyperspectral imaging for detecting fecal and ingesta contaminants on poultry carcasses. *Transactions of the ASAE, 45*(6), 2017–2026.

Qin, J., & Lu, R. (2006). Hyperspectral diffuse reflectance for rapid, noncontact determination of the optical properties of turbid materials. *Applied Optics, 45*, 8366–8373.

USDA. (1996). Pathogen reduction: hazard analysis and critical control point (HACCP) systems: Final rule. *Federal Register, 61*, 38805–38989.

USDA. (1997). HACCP-based inspection models project (HIMP): Proposed rule. *Federal Register, 62*, 31553–31562.

USDA. (2005). Poultry products inspection regulations. 9 CFR 381.76. *Code of Federal Regulations, 9*(2), 456–465.

USDA. (2008). *Poultry Production and Value—2007 Summary*. Washington, DC: National Agricultural Statistics Service.

Yang, C. C., Chao, K., Chen, Y. R., & Early, H. L. (2005). Systemically diseased chicken identification using multispectral images and region of interest analysis. *Computers and Electronics in Agriculture, 49*(2), 255–271.

Yang, C. C., Chao, K., & Chen, Y. R. (2005). Development of multispectral imaging processing algorithms for food safety inspection on poultry carcasses. *Journal of Food Engineering, 69*(2), 225–234.

Yang, C. C., Chao, K., Chen, Y. R., Kim, M. S., & Early, H. L. (2006). Simple multispectral image analysis for systemically diseased. *Transactions of the ASAE, 49*(1), 245–257.

Yang, C. C., Chao, K., & Kim, M. S. (2009). Machine vision system for online inspection of freshly slaughtered chickens. *Sensing and Instrumentation for Food Quality and Safety, 3*(1), 70–80.